Advanced Materials Science

Research Article

ISSN: 2398-6883

Tuning the structural and the magnetic properties of BiFeO3 magnetic nanoparticles

Makridis A[1,2]*, Myrovali E[1,2], Sakellari D[1,2] and Angelakeris M[1,2]

[1]School of Physics, Faculty of Sciences, Aristotle University of Thessaloniki, 54124 Thessaloniki, Greece

[2]Center for Interdisciplinary Research and Innovation (CIRI-AUTH), 57001 Thessaloniki Greece

Abstract

The explosive expansion of multiferroics' literature in recent years demonstrates the fast-growing interest in this field. Bismuth ferrite is one of the most extensively investigated multiferroic magneto-electric compounds that possesses anti-ferromagnetic and ferroelectric properties in room temperature. In this study, aqueous coprecipitation method is followed together with an annealing step at 700°C to form bismuth ferrite nanoparticles. The investigation of the impact of the final's product Bi/Fe ratio on its structural as well as on its magnetic properties is one of the key issues of this work. Furthermore, the presence of impurity phases in the final bismuth oxide product may be controlled by simple synthetic modifications as proposed. At the same time, structural and magnetic properties of as prepared and post-synthesis annealed bismuth iron oxide samples reveal the significance of calcination on forming $BiFeO_3$ single-phase nanoparticles, diminishing secondary bismuth oxide phases, crucial feature to bring out the unique multi-electric properties.

Introduction

Materials that simultaneously possess two or more ferroic order parameters, have become a hot topic of research in recent years [1,2]. The link between magnetic and electric properties potentially allows the creation of novel devices if magnetic and electric order can be mutually controlled. Among the different types of multiferroic compounds, bismuth ferrite ($BiFeO_3$) stands out because it is perhaps the only one exhibiting both anti-ferromagnetic and ferroelectric properties, observed at room temperature [1-4]. Therefore, during the past decade, extensive research has been devoted to bismuth iron oxide (BFO) -based materials in a variety of forms, including ceramic bulks, thin films and nanostructures [1].

Primarily, $BiFeO_3$–based materials are of interest as multiferroics used for the development of magnetoelectric materials and photovoltaics, including thin film materials, nanostructures and compounds with $BiFeO_3$ nanosized blocks [4,5] and more recently of multifunctional agents being able to simultaneously act as sensitizers for radiotherapy as well as heat mediators for hyperthermia [5]. Although, multiple reviews report on the synthesis of $BiFeO_3$, which is regarded as an equilibrium compound [1,2], by applying different methods and determining the optimal conditions for producing this compound free from impurity phases, a pure single-phase product still remains a hard task to achieve [1]. The synthesis metastability was proposed as a reason for the inability to acquire this compound uncontaminated from secondary bi-products of the Bi_2O_3–Fe_2O_3 system [1]. Moreover, additional constraints for the success of a solid phase synthesis process may be attributed to non-stoichiometry and variations in the homogeneity region with increased temperature [1]. Meanwhile, the activation of $BiFeO_3$ formation seems to depend on the chemical background of the initial mixture [1]. In this case, several subsequent transformations occur when $BiFeO_3$ is synthesized from Bi_2O_3 and Fe_2O_3 by the solid-state chemical reaction method. Thus, at the initial stage, the formation of $Bi_{25}FeO_{39}$ takes place with its maximum quantity recorded at 500°C. Then, $BiFeO_3$ synthesis intensifies sharply at about 600°C, and the further increase in the reaction temperature leads to the formation of $Bi_2Fe_4O_9$ along with $BiFeO_3$ and $Bi_{25}FeO_{39}$ phases. The tendency of $Bi_2Fe_4O_9$ and $Bi_{25}FeO_{39}$ formation during $BiFeO_3$ synthesis depended on the quality of the initial reagents [1]. Insufficiently pure precursors resulted in the formation of these secondary phases and to their stable occurrence as impurities during $BiFeO_3$ formation. Eventually, the difficulty to synthesize single-phase $BiFeO_3$ may derive from the fact that $Bi_2Fe_4O_9$ and $Bi_{25}FeO_{39}$ are thermodynamically more stable than $BiFeO_3$ [1,2].

Various synthetic attempts of variable in size and morphology $BiFeO_3$ nanoparticles (NPs) are examined, including low temperature techniques, such as the hydrothermal and coprecipitation method together with subsequent annealing stage [1, 5-28]. The choice of the precursors has direct impact on the formation, structure and size of $BiFeO_3$ [4,5]. Hardy *et al.* [28] reported that $BiFeO_3$ crystallization begins around 400°C, an increase in the reaction temperature of up to 500–60°C may yield single-phase $BiFeO_3$. On the other hand, Mikhailov *et al.* [4] concluded, after thermodynamic calculations, that the synthesis temperature to produce single-phase $BiFeO_3$ should not be above 727°C, that is, above the temperature of the α→ Bi_2O_3 transition, as the high entropy of the disordered β-Bi_2O_3 sharply decreases the Gibbs energy of bismuth ferrite formation. The suggested optimal synthesis temperature is around 720°C. Despite, the numerous attempts to synthesize $BiFeO_3$ NPs, final product is a multiphase micro

Correspondence to: Makridis A, School of Physics, Faculty of Sciences, Aristotle University of Thessaloniki, 54124 Thessaloniki, Greece, E-mail: anmakrid@physics.auth.gr

Key words: *bismuth ferrite, BiFeO3, multiferroic, magnetoelectric, coprecipitation*

Received: October 17, 2019; **Accepted:** November 22, 2019; **Published:** November 25, 2019

or nano -powder, with no distinct reasoning for the multiple phases' formation during $BiFeO_3$ synthesis [4-8].

In this work, aqueous coprecipitation method is proposed as a first synthesis stage and followed by two hours annealing stage, under A_r atmosphere at 700°C, temperature approximating the optimal calcination temperature to form single-phase $BiFeO_3$ NPs. The role of Bi/Fe ratio impact to the final BFO product and its structural and magnetic properties is the first step of our work. Furthermore, we examine how the presence of impurity phases in the final BFO product can be controlled by a facile synthesis modification such as the precursor replacement. At the same time, the impact of the sintering process occurring during annealing stage is extensively studied by correlation of structural and magnetic features.

Materials and methods

Synthesis

All chemicals were purchased from Riedel-De Haen, VWR Chemicals, AnalR Normapur and PanReac-AppliChan chemicals companies. Six BFO NPs samples were prepared by aqueous co-precipitation method and all chemicals reagents used in the following synthesis experiments were of high purity without any further purification. The first four samples were prepared using Hydrochloric acid (H_2O:HCl 37%), whereas the fifth and the sixth one had nitric acid [H_2O:HNO_3 65%] instead. Samples' notation together with their structural and magnetic features appears in Table 1.

The role of Bi/Fe molar ratio

To synthesize BFO1 sample, 0.83 g of bismuth nitrate pentahydrate ($Bi(NO_3)_3{\cdot}5H_2O$) and 2 g of iron nitrate nonahydrate ($Fe(NO_3)_3{\cdot}9H_2O$) were dissolved in 150 mL of distilled water, keeping the Bi/Fe molar ratio at 1/3.

For the synthesis of BFO2 sample, 7.47 g of bismuth nitrate pentahydrate ($Bi(NO_3)_3{\cdot}5H_2O$) and 2 g of iron nitrate nonahydrate ($Fe(NO_3)_3{\cdot}9H_2O$) were dissolved in 150 mL of distilled water, keeping the Bi/Fe molar ratio at 3/1.

The target for the third sample (BFO3) was to prepare BFO NPs with molar ratio 1/1. For this reason, 2.5 g of bismuth nitrate pentahydrate ($Bi(NO_3)_3{\cdot}5H_2O$) and 2 g of iron nitrate nonahydrate ($Fe(NO_3)_3{\cdot}9H_2O$) were dissolved in 150 mL of distilled water.

In all samples, since stirring did not result to a clear solution, 20 mL of HCl (37%) were added to form a transparent solution. The pH of the solutions was controlled by immediately adding drops of 1 M NaOH solution, until the desired value 12 was reached. Temperature was kept constant at 84°C in all three synthesis attempts. The precipitated orange colored products were kept at T_r for about 24 h and were washed 5 times with distilled water to remove non-reacting excesses. The final powder products were annealed at A_s atmosphere at 700°C for 2 h.

Table 1. Structural and magnetic properties of BFO samples

Samples	(Synthesis) Molar ratio (Bi/Fe)	(SEM) Atomic ratio (Bi/Fe)	(XRD) Size (nm)	M_s (Am^2/kg)	H_c (mT)
BFO1	1/3	0.6	29.0±9.5	5.30	14.0
BFO2	3/1	5.4	21.0±4.5	0.00	0.5
BFO3	1/1	1.7	19.0±3.2	0.40	5.0
BFO4	1/1	1.8	42.0±6.3	0.20	20.0
BFO5	1/1	1.4	38.0±12.3	0.20	32.0
BFO6	1/1	1.6	34.0±9.9	0.05	0.2

The role of the precursor

A fourth synthesis was also attempted (BFO4 sample), where the molar ratio was kept at 1/1 and this was the last sample that hydrochloric acid (H_2O:HCl) was used as synthesis acid. For the preparation of this sample, 7.76 g of bismuth nitrate pentahydrate ($Bi(NO_3)_3{\cdot}5H_2O$) and 6.46g of iron nitrate nonahydrate ($Fe(NO_3)_3{\cdot}9H_2O$) were dissolved in 150 mL of distilled water. As obtained in previous samples, stirring did not result to a clear solution. For that reason, 35 mL of HCL (37%) were added to form a transparent solution. 1 M of NaOH solution was then added drop by drop wise until a pH of 10 was reached while temperature was kept constant at 70°C. The precipitated orange colored product was kept at T_r for about 24 h and was washed 5 times with distilled water to remove unreactant products. These powders were annealed at A_r atmosphere at 700°C for 2 h.

To synthesize the fifth BFO sample (BFO5 sample), nitric acid [HNO_3] was used during preparation of the sample, instead of hydrochloric acid [H_2O:HCl]. Meanwhile, stronger base solution of NaOH (2 M) was added in this synthesis procedure instead of the weaker NaOH (1 M) base solution, as mentioned above in all previous samples. Concerning the synthesis procedure, 2 g of bismuth nitrate pentahydrate ($Bi(NO_3)_3{\cdot}5H_2O$) were dissolved in 100 mL of distilled water. Solution was kept under stirring and at a constant temperature of 70°C. Afterwards, nitric acid [HNO_3] (65%) was added into the solution, until it became transparent. Separately, 1.66 g of iron nitrate nonahydrate ($Fe(NO_3)_3{\cdot}9H_2O$) were added into 50 mL of distilled water. The two solutions were then mixed, while temperature was constant at 70°C, under mild stirring. At that time, NaOH (2 M) solution was added drop by drop, until pH reached the value 12. Solution was kept under continuous stirring and at a temperature of 70°C for 20 min. Moreover, four washes were done with distilled water and the orange-brown product was left overnight to dry. The last step of the preparation was annealing under A_r atmosphere at 700°C for 2 h.

The synthesis properties of sample BFO6 are the same as BFO5 sample, without the annealing process. This sample is used as a reference sample for the purposes of this work.

Methods

X-Ray-diffraction patterns were obtained using a Philips PW 1710 diffractometer with CuKα as a radiation source ($\lambda = 1.54242$ Å) in the 2θ range from 20° to 90° with scanning step width of 0.05° and 3 s scanning time per step. The structural observation and micro-morphology were conducted with a JEOL JSM 840A SEM, scanning electron microscopy (SEM) equipped with an OXFORD INCA energy dispersive X-ray analyzer (EDS) for elemental analyses to measure Bi/Fe atomic ratios. The magnetization hysteresis curves (M vs H) at room temperature were obtained by vibrating sample magnetometry (VSM – 1.2H/CF/HT Oxford Instruments VSM).

Results and discussion

Nanoparticle features

BFO nanoparticles were prepared by precise controls of a typical aqueous co-precipitation method. This work's first target is to determine the adequate, from structural point of view, Bi/Fe molar ratio, since multiferroic NPs possess optimum magnetoelectric properties when stoichiometric bismuth iron oxide phase ($BiFeO_3$) dominates in their structure [4-17]. In order to examine how different stoichiometry may affect the structural and magnetic properties of $BiFeO_3$ NPs, three different synthetic protocols were followed, aiming to three different

Bi/Fe molar ratios, 1/3 in sample BFO1, 3/1 in sample BFO2 and 1/1 in sample BFO3, as presented in Table 1.

Figure 1 shows the corresponding XRD patterns for post-synthetic annealed samples where in Figure 1a, from bottom to top we have: red: BFO1, green: BFO2 and blue: BFO3 patterns corresponding to 1/1 1/3 and 3/1 Bi/Fe ratios respectively. In all cases, the peaks coincide with the reference ones for BFO ($BiFeO_3$:PDF #20-0169, olive color vertical lines). Additional peaks can be attributed to secondary phases formed in the fabrication process (BiOCl:PDF#06-0249 grey color peaks) apparent in all 3 samples (mainly in BFO2) while in BFO1 and BFO3 samples the non-stoichiometric bismuth iron oxide phases also exist, i.e. $Bi_2Fe_4O_9$:PDF #25-0090 and $Bi_{46}Fe_2O_{72}$:PDF#20-0170 for sample BFO1 and $Bi_2Fe_4O_9$:PDF#25-0090 for sample BFO3. The existence of BiOCl phase may be attributed to the hydrochloric acid used during the synthesis. Meanwhile, the desirable stoichiometric $BiFeO_3$ phase (main reference peaks are colored as olive color lines- $BiFeO_3$: PDF#20-0169) exists in all five samples. Regarding the samples synthesized with different Bi/Fe stoichiometry (BFO1, BFO2, BFO3), $BiFeO_3$ phase appears to be as a secondary phase with more intense in BFO3 sample (blue curve with 1/1 Bi/Fe nominal ratio).

On the other hand, the presence of bismuth iron oxide phases such as $Bi_{25}FeO_{40}$ (PDF#46-0416), $Bi_{46}Fe_2O_{72}$ (PDF#20-0170) and $Bi_2Fe_4O_9$ (PDF#25-0090) may be attributed on the kinetics of formation, due to which, some impurity phases are always obtained along with the stoichiometric $BiFeO_3$ phase (PDF#20-0169), as the major phase during the synthesis of BFO MNPs. Such impurity phases exist in multiple relevant reports [4,5,17,22,26].

Keeping the Bi/Fe molar ratio 1/1 as the optimum synthesis ratio to prepare multiferroic NPs, this study's second goal is to examine the impact of the base solution as well as of the type of acid used during synthesis on the final NPs phase. More specifically, it is examined if the undesirable phases of BiOCl and of the nonstoichiometric bismuth oxides can be avoided at the final products by replacing hydrochloric acid with nitric acid during synthesis.

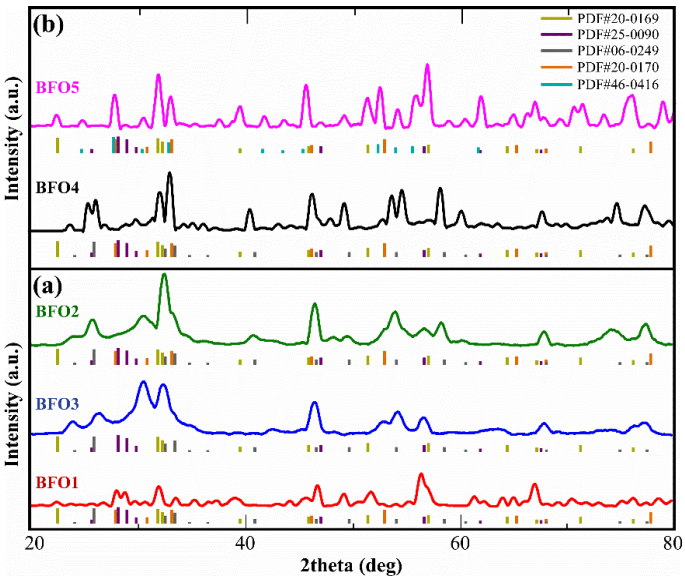

Figure 1. X-ray diffractograms of BFO samples synthesized a) using different nominal Bi/Fe molar ratio under the same synthesis conditions (red: BFO1 (1/3), green: BFO2 (3/1) and blue: BFO3 (1/1)) and b) using the same nominal Bi/Fe ratio 1/1 under different synthesis conditions (black: BFO4 (hydrochloric acid + weak base), pink: BFO5 (nitric acid + strong base) all annealed at 700 °C for 2 h under A_r atmosphere

As Figure 1b shows, using nitric acid (used in sample BFO5) instead of hydrochloric acid (used in BFO1, BFO2, BFO3 and BFO4 samples) during synthesis, appears to act beneficially to the structure of BFO5 sample, since bismoclite phase (BiOCl PDF#06-0249 grey color peaks) no longer appears (BFO5 sample comparing with BFO1, BFO3, BFO2 and BFO4 samples). Additionally, by comparing BFO4 and BFO5, samples with the same Bi/Fe nominal ratio but differences in synthesis precursors, one can observe that stoichiometric $BiFeO_3$ phase (PDF#20-0169) is dominant in BFO5 sample. Bismuth iron oxides phases ($Bi_{25}FeO_{40}$:PDF #46-0416, $Bi_{46}Fe_2O_{72}$:PDF#20-0170 and $Bi_2Fe_4O_9$: PDF#25-0090) recorded here as secondary phases as well, in contrast with sample BFO_4 where $BiFeO_3$ appears to be as secondary phase. Bismoclite (BiOCl: PDF#06-0249 grey color peaks) presented in BFO4 sample as the dominant phase with the non-stoichiometric bismuth iron oxide phases ($Bi_{46}Fe_2O_{72}$:PDF#20-0170 and $Bi_2Fe_4O_9$: PDF#25-0090) exist also as secondary phases.

Figure 2a shows the X-ray diffractograms of the annealed BFO sample (BFO5) in nominal Bi/Fe molar ratio (1/1) together with its as prepared reference sample (BFO6). Regarding the not annealed reference sample BFO6, the presence of bismuth oxide phases (Bi_2O_3: PDFs #45-1344 and #51-1161) is unavoidable as clearly shown with blue and green vertical lines, under spectra (Figure 2a), respectively. On the contrary, the desirable target phase of bismuth iron oxide ($BiFeO_3$) is dominant (PDF#20-0169- olive colored lines) without any presence of bismuth oxides after 2 h annealing under A_r atmosphere at calcination temperature of 700°C.

Microstructural characterization of the multiferroic samples, performed by a droplet of 1 mg/mL solution upon a silicon substrate is depicted in Figures 2b and 2c, SEM images of the prepared BFO samples before (BFO6- Figure 2b left brown color box) and after (BFO5- Figure 2c right pink color box) annealing. Interestingly, large (>1μm in diameter) multifaceted particles were observed before annealing (BFO6 samples) while smaller (<1μm in diameter) cubic-like particles with smoother faces and clearer edges, are formed after 2 h annealing at 700°C at A_r atmosphere (BFO5 sample). Similar effects of annealing on morphology has been reported, previously in for 600°C annealing temperature. This difference in morphology between before and after annealed samples (BFO6 and BFO5 samples, respectively) may be attributed to the diminishing of the secondary impurity Bi oxide phases (Bi_2O_3) blocking the domination of single-phase NPs. It is reported most often that $BiFeO_3$ is accompanied by secondary phases such as $Bi_2Fe_4O_9$ and $Bi_{25}FeO_{29}$ [4,5] The impurity phases in the XRD patterns could be attributed to the volatilization of Bi^{3+} ions which resulted due to excess addition of Bi.

By measuring the full width at half maximum of the 4 strongest diffractions peaks and using Scherrer's formula, the samples crystallite sizes were estimated to be 19–42 nm as shown in Table 1. Elemental analysis with EDX detection revealed the Bi/Fe atomic ratio for each sample as summarized in Table 1 in comparison with the respective initial Bi/Fe molar ratio used in the synthesis. As it is expected, BFO1 sample with initial Bi/Fe molar ratio at 1/3 has the highest Fe content with 0.61 Bi/Fe atomic ratio. On the contrary, initial Bi/Fe molar ratio of 3/1 and 1/1, used in samples BFO2 and BFO3, BFO4, BFO5, BFO6, respectively, resulted to a Bi content excess as shown in third column of Table 1. Interestingly, bismuth atomic content in BFO2 sample is more than five times greater than iron atomic content (Bi/Fe atomic ratio is 5.4 as shown in Table 1), explaining the strong existence of the bismuth enhanced impurity phase of $Bi_{46}Fe_2O_{72}$ (PDF#20-0170). It should be noticed that this deviation from 1/1 Bi/Fe atomic ratio

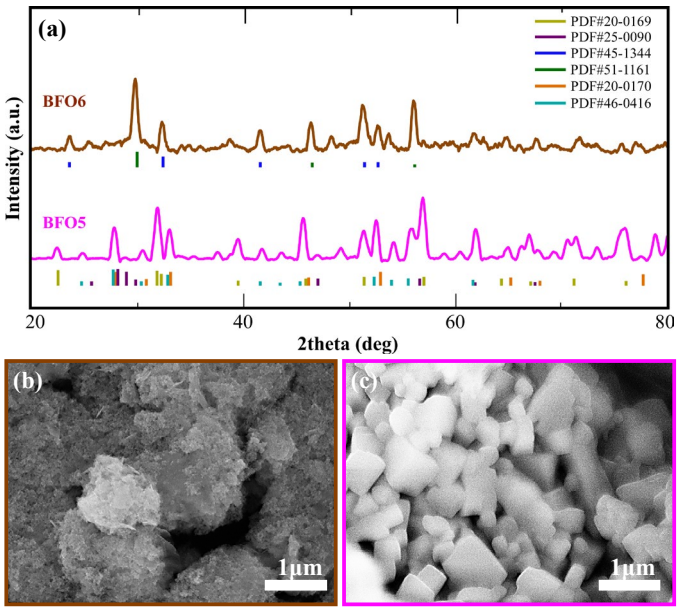

Figure 2. (a) X-ray diffractograms of the annealed BFO sample (BFO5) in nominal Bi/Fe molar ratio (1/1) together with its reference sample (BFO6) before annealing. SEM images of the two samples (b) BFO6 demonstrating the change in morphology after the 2 h calcination at 700 °C under A_r atmosphere and (c) BFO5

in BFO3, BFO4, BFO5 and BFO6 samples can explain the several secondary phases that XRD results revealed (Figure 1 and Figure 2a) for these samples. Additionally, BFO5 sample has the closer to 1/1 Bi/Fe atomic ratio (1.4) comparing with the other three nominal 1/1 Bi/Fe molar ratio samples (BFO3, BFO4 and BFO6 with 1.7, 1.8 and 1.6 Bi/Fe atomic ratios, respectively) and this explains why, regarding to the XRD results, the stoichiometric phase of $BiFeO_3$ (PDF#20-0169-olive colored lines in Figures 1 and 2a) is presented as the dominant phase in this sample. It should be mentioned here that even though BFO3 and BFO4 samples have similar atomic Bi/Fe ratios (1.7 and 1.8, as shown in Table 1, respectively) their crystallite sizes are strongly different (BFO4 NPs have a twice larger crystallite size (42 nm) than BFO3 (19 nm). This may be attributed to the difference in temperature reaction during synthesis (83°C and 70°C in case of BFO3 and BFO4 sample synthesis respectively) as well as to the pH level reached in each case (12 and 10 for BFO3 and BFO4 samples, respectively). It has been shown [26-37], that pH level during the synthesis of BFO NPs has direct impact on their size but it is worth mentioning here that there is a lack of literature works on this connection. Meanwhile, most literature reports, focusing on the synthesis of BFO NPs, use pH synthesis values up to 11 which is less that pH 12 that used for the preparation of BFO3 sample [26,35,37]. Additionally, annealing temperature appears in several works as the most crucial synthesis factor strongly affecting the size of BFO NPs [37]. Regrading Figure 1, one can state also that the presence of secondary Bi iron oxide phases is more evident in BFO4 than in BFO3, which is a result of the different synthesis parameters followed as discussed before and can be also a reason of the observed size difference.

To investigate the magnetic properties of the BFO particles, magnetic measurements were performed using VSM magnetometry. The magnetic response observed as a function of the applied magnetic field is correlated with the structural findings while the magnetic features (saturation magnetization M_s and coercive field H_c) of each sample are outlined in the last two columns of Table 1. Figure 3 presents the magnetization as a function of the applied magnetic field (field range of ±1 T) of the BFO powders at room temperature, also well known as magnetization hysteresis loop.

As it is summarized in Table 1 and also shown in Figures 3a and 3b, BFO samples with Bi excess (Bi/Fe atomic ratio > 1 in samples BFO2, BFO3, BFO4, BFO5, BFO6) present weaker saturation magnetization at 1 T (up to 0.4 Am^2/kg) with respect to sample BFO1 appearing as the magnetically strongest (M_s=5.3 Am^2/kg), in accordance with its Fe content excess (Bi/Fe atomic ratio = 0.6). Regarding the samples' coercivity, Figures 3b and 3d show that BFO2 and BFO6 samples have the weakest coercive field among all samples, 0.5 and 0.2 mT, respectively. Meanwhile, the excess in Bi content (Bi/Fe atomic ratio equals to 5.4) in BFO2 sample favors a diamagnetic-like behavior, as the corresponding green curve in Figure 3a presents. As far as the reference, not annealed BFO6 sample concerns, the presence of Bi oxide phases (blue and green peak-corresponded lines in Figure 2a can explain its weak M_s and H_c values (orange curves in Figures 3c and 3d). In case of BFO5 sample, after the annealing process, the improvement of its phase (the unfavorable bismuth oxide phases of BFO6 sample no longer exist in BFO5, as XRD results shown in Figure 2a) directly affects its magnetic features.

Interestingly, BFO5 sample presents a coercivity of 32 mT and an M_s of 0.2 Am^2/kg for a crystallite size of 38 nm. Analogous magnetic behavior with the best, from structural point of view sample (as in the case of BFO5), has been also been reported [37]. More specifically, Park *et al.* shown in their work that $BiFeO_3$ MNPs of 41 nm (comparable to BFO5 sample's size of 38 nm) possessed a coercive field value of 30.5 mT, which is very similar to BFO5 sample's coercivity. Additionally, similar saturation magnetization to BFO5 sample has been reported in Carranza-Celis *et al.* work [17]. More specifically, in that work, sol gel synthesis method was used to form BFO NPs that annealed at 600°C. Room temperature hysteresis loop exhibited superparamagnetic-like behavior with a very weak ferromagnetic component, with a 2.2 mT coercive field and similar to BFO5 M_s at 0.17 Am^2/kg. It should be noted here that different synthesis procedure may impact the final structural and magnetic properties of the products. More specifically, Carranza-Celis *et al.* suggest in their work [17] that annealing temperature may

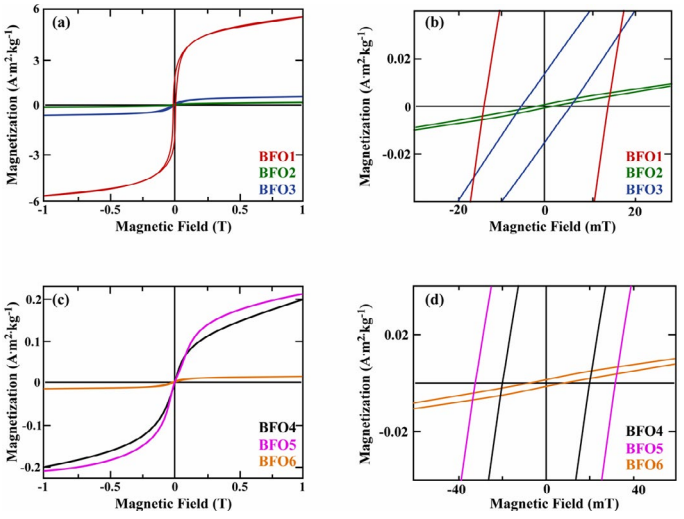

Figure 3. Hysteresis loops at 300 K for (a) BFO samples synthesized using different nominal Bi/Fe molar ratio (BFO1 (1/3), BFO2 (3/1) and BFO3 (1/1)) and annealed at 700 °C for 2 h and (c) BFO samples synthesized using different precursors, under the same nominal Bi/Fe molar ratio (1/1) with BFO4 and BFO5 annealed at 700 °C under A_r atmosphere for 2 h and with reference as-prepared BFO6 sample. (b) and (d) with rescaled axis depict the respective coercivity for all samples

have a crucial impact not only to the structure of the BFO NPs but to their magnetic properties as well. Interestingly, after applying linear extrapolation on their experimental magnetization data, Park *et al.* [37-43] suggest that the highest magnetization achievable for substrate-free $BiFeO_3$ NPs, ranging in size diameter from 14 to 75 nm, can attain values of up to about 1.82 Am^2/kg. To put this value into context, magnetization values of 1.00-1.66 Am^2/kg for epitaxially grown $BiFeO_3$ thin films have been previously reported [4,5]. It is well known from literature that the secondary phases in BFO NPs can also affect their magnetic properties [4,5] and it has been extensively mentioned that is impossible to avoid them at the final product [5]. Although the weak M_s value of BFO5 NPs sample, which can be attributed to the coexisted secondary Bi iron oxide phases and the excess in Bi content, its structural and magnetic properties are obviously improved compared with the rest 1/1 Bi/Fe samples prepared for the purposes of this work, indicating that the exploration of each synthesis parameter may lead to the BFO sample with improved structural and magnetic properties.

Conclusions

$BiFeO_3$ NPs were formed by using aqueous coprecipitation method followed by 2 h annealed at A_r atmosphere at 700°C. The investigation of three different Bi/Fe molar ratios (1/3, 3/1, 1/1) and their impact to the final BFO product highlights the 1/1 as the optimum, both from structural and magnetic point of view, Bi/Fe ratio. Furthermore, the occurrence of impurity phases in the final BFO product can be avoided by simple synthesis precursors replacement. At the same time, structural and magnetic properties of not-annealed and post annealed BFO samples reveal the significance of annealing procedure on forming $BiFeO_3$ without the presence of bismuth oxide phases which is crucial to bring out the unique magneto-electric properties.

Acknowledgements

This research is funded in the context of the project "Exploitation of field effects on appropriate nanoparticulate carriers for modern biomedical applications" (MIS 5005039) under the call for proposals "Supporting researchers with emphasis on new researchers" (EDULLL 34). The project is co-financed by Greece and the European Union (European Social Fund- ESF) by the Operational Programme Human Resources Development, Education and Lifelong Learning 2014-2020.

References

1. Martin LW, Crane SP, Chu YH, Holcomb MB, Gajek M, et al. (2008) Multiferroics and magnetoelectrics: thin films and nanostructures. *Journal of Physics: Condensed Matter Condensed Matter* 20: 434220.
2. Fiebig M, Lottermoser T, Meier D, Trassin M (2016) The evolution of multiferroics. *Nature Reviews Materials 1*: 16046.
3. Catalan G, Scott JF (2009) Physics and applications of bismuth ferrite. *Advanced materials* 21: 2463-2485.
4. Rojac T, Bencan A, Malic B, Tutuncu G, Jones JL, et al. (2014) BiFeO3 Ceramics: Processing, electrical, and electromechanical properties. *Journal of the American Ceramic Society* 97: 1993-2011.
5. Wang JBNJ, Neaton JB, Zheng H, Nagarajan V, Ogale SB, et al. (2003) Epitaxial BiFeO3 multiferroic thin film heterostructures. *science* 299: 1719-1722.
6. Teague JR, Gerson R, James WJ (1970) Smart materials for energy, communications and security. *Solid State Communications* 8: 1073-1074.
7. Wu J, Fan Z, Xiao D, Zhu J, wang J, et al. (2016) A flexible quasi-solid-state nickel–zinc battery with high energy and power densities based on 3D electrode design. *Progress in Materials Science* 84: 335-402.
8. Wang YP, Yuan GL, Chen XY, Liu JM, Liu ZG, et al. (2006) Electrical and magnetic properties of single-phased and highly resistive ferroelectromagnet BiFeO3 ceramic. *Journal of Physics D: Applied Physics* 39*:* 2019.
9. Choi T, Lee S, Choi YJ, Kiryukhin V, Cheong SW, et al. (2009) Insulating interlocked ferroelectric and structural antiphase domain walls in multiferroic YMnO3. *Science* 324: 63-66.
10. Pyatakov AP, Zvezdin AK (2012) Inhomogeneous magnetoelectric interaction in multiferroics and related new physical effects. *Physics-Uspekhi* 55: 557.
11. Li S, Nechache R, Harnagea C, Nikolova L, Rosei L (2012) Photovoltaic properties of Bi2FeCrO6 epitaxial thin films. *Applied Physics Letters* 101: 192903.
12. Rajaee A, Wensheng X, Zhao L, Wang S, Liu Y, et al. (2018) Multifunctional BISMUTH FERRITE NANOPARTICLES AS MAGNETIC LOCALIZED DOSE ENHANCEMENT IN RADIOTHERAPY AND IMAGING. *Journal of biomedical nanotechnology* 14: 1159-1168.
13. Maitre A, Francois M, Gachon JC (2004) Experimental study of the Bi2O3-Fe2O3 pseudo-binary system. *Journal of Phase Equilibria and Diffusion* 25: 59-67.
14. Haumont R, Saint-Martin R, Byl C (2008) Centimeter-size BiFeO3 single crystals grown by flux method. *Phase Transitions* 81: 881-888.
15. Silva J, Reyes A, Esparza H, Camacho H, Fuentes L, et al. (2011) BiFeO3: A review on synthesis, doping and crystal structure. *Integrated Ferroelectrics* 126: 47-59.
16. Lu J, Qiao LJ, Fu PZ, Wu YC (2018) Phase equilibrium of Bi2O3-Fe2O3 pseudo-binary system and growth of BiFeO3 single crystal. *Journal of Crystal Growth* 318: 936-941.
17. Carranza-Celis D, Cardona-Rodríguez A, Narvaez J, Moscoso-Londono O, Muraca D, et al. (2019) Ramírez control of multiferroic properties in BiFeO3 nanoparticles. *Scientific reports* 9: 3182.
18. Morozov MI, Lomanova NA, Gusarov VV (2003) Specific features of BiFeO3 formation in a mixture of bismuth (III) and iron (III) oxides. *Russian Journal of General Chemistry* 73: 1676-1680.
19. Valant M, Axelsson AK, Alford N (2007) Peculiarities of a solid-state synthesis of multiferroic polycrystalline BiFeO3. *Chemistry of Materials* 19*:* 5431-5436.
20. Selbach SM, Einarsrud MA, Grande T (2008) On the thermodynamic stability of BiFeO3. *Chemistry of Materials* 21: 169-173.
21. Phapale S, Mishra R, Das D (2008) Standard enthalpy of formation and heat capacity of compounds in the pseudo-binary Bi 2O 3-Fe 2O 3 system. *Journal of Nuclear Materials* 373: 137-141.
22. Lomanova NA, Gusarov VV (2013) Influence of synthesis temperature on bifeo 3nanoparticles formation. *Наносистемы: физика, химия, математика 4*.
23. Xu JH, Ke H (2009) Graphene oxide nano-sheets on structural, morphological and photocatalytic activity of BiFeO3-based nanostructures. *Journal of Alloys and Compounds* 472: 473-477.
24. Liu, Hu B, Du Z (2011) Hydrothermal synthesis and magnetic properties of single-crystalline BiFeO3 nanowires. *Chemical Communications* 47: 8166-8168.
25. Gajović A, Sturm S, Jančar B, Šantić A, (2010) The synthesis of pure-phase bismuth ferrite in the Bi–Fe–O system under hydrothermal conditions without a mineralizer. *Journal of the American Ceramic Society* 93: 3173-3179.
26. Muneeswaran M, Jegatheesan P, Giridharan (2013) Synthesis of nanosized BiFeO3 powders by co-precipitation method. *Journal of Experimental Nanoscience* 8: 341-346.
27. Popa M (2007) Synthesis and structural characterization of single-phase BiFeO3 powders from a polymeric precursor. *Journal of the American Ceramic Society 90*: 2723-2727.
28. Hardy S (2011) Effects of precursor chemistry and thermal treatment conditions on obtaining phase pure bismuth ferrite from aqueous gel precursors Mullens. *Journal of the European Ceramic Society* 29: 3007-3013.
29. Mikhailov AV, Gribchenkova NA (2011) Mass spectrometric investigation of vaporization in the Bi2O3-Fe2O3 system. *Russian Journal of Physical Chemistry A* 85: 26-30.
30. Shetty S (2002) Size effect study in magnetoelectric BiFeO3 system 58: 1027-1030.
31. Yang J (2011) Electrochemical performances of Co-doped LiFePO4/C obtained by hydrothermal method. *Journal of Alloys and Compounds* 509: 9271-9277.
32. Prado-Gonjal J (2009) Microwave–hydrothermal synthesis of the multiferroic BiFeO3 *Materials Research Bulletin* 44: 1734-1737.
33. Kothai V (2012) Synthesis of BiFeO 3 by carbonate precipitation. *Bulletin of Materials Science* 35: 157-161.

34. Jurca C (2009) Starch–A suitable fuel in new low-temperature combustion-based synthesis of zinc aluminate oxides. *Journal of Thermal Analysis and Calorimetry* 97*:* 91-98.

35. Huang F (2013) Peculiar magnetism of BiFeO3 nanoparticles with size approaching the period of the spiral spin structure. *Scientific Reports 3*: 2907.

36. Sosnowska I (2002) Crystal structure and spiral magnetic ordering of BiFeO3 doped with manganese. *Applied Physics A* 74: 1042.

37. Park TJ (2007) Size-dependent magnetic properties of single-crystalline multiferroic BiFeO3 nanoparticles. *Nano Letters* 7: 766-772.

38. Sosnowska TP (1982) Spiral magnetic ordering in bismuth ferrite. *Journal of Physics C: Solid State Physics* 15: 4835.

39. Srinivas V, Raghavender AT, Kumar KV (2016) Structural and magnetic properties of Mn doped BiFeO3 nanomaterials. *Physics Research International* 3: 5.

40. Eerenstein W, Morrison FD, Dho J, Blamire MG, Scott JF (2005) Comment on "Epitaxial BiFeO3 multiferroic thin film heterostructures. Mathur *Science* 307: 1203-1203.

41. Bea H, Bibes M, Barthélémy A, Bouzehouane K, Jacquet E, et al. (2005) Tunnel magnetoresistance and robust room temperature exchange bias with multiferroic BiFeO3 epitaxial thin films. *Applied Physics Letters* 87: 072508.

42. Ederer, Spaldin NA (2005) Influence of strain and oxygen vacancies on the magnetoelectric properties of multiferroic bismuth ferrite. *Physical Review B* 71: 224103.

43. Berbenni V, Milanese C, Bruni G, Girella A (2015) Structural and magnetic properties of Mn doped BiFeO3 nanomaterials. *Ceramics International* 41: 7216-7220.